无网格粒子类方法专题

基于分区径向基函数配点法的大变形分析[1)]

王莉华 [*,2)]　李溢铭 [*]　褚福运 [†]

[*](同济大学航空航天与力学学院, 上海 200092)

[†](上海宇航系统工程研究所, 上海 201109)

摘要　无网格法因为不需要划分网格, 可以避免网格畸变问题, 使得其广泛应用于大变形和一些复杂问题. 径向基函数配点法是一种典型的强形式无网格法, 这种方法具有完全不需要任何网格、求解过程简单、精度高、收敛性好以及易于扩展到高维空间等优点, 但是由于其采用全域的形函数, 在求解高梯度问题时存在精度较低和无法很好地反应局部特性的缺点. 针对这个问题, 本文引入分区径向基函数配点法来求解局部存在高梯度的大变形问题. 基于完全拉格朗日格式, 采用牛顿迭代法建立了分区径向基函数配点法在大变形分析中的增量求解模式. 这种方法将求解域根据其几何特点划分成若干个子域, 在子域内构建径向基函数插值, 在界面上施加所有的界面连续条件, 构建分块稀疏矩阵统一求解. 该方法仍然保持超收敛性, 且将原来的满阵转化成了稀疏矩阵, 降低了存储空间, 提高了计算效率. 相比较于传统的径向基函数配点法和有限元法, 这种方法能够更好地反应局部特性和求解高梯度问题. 数值分析表明该方法能够有效求解局部存在高梯度的大变形问题.

关键词　无网格, 分区径向基函数配点法, 大变形, 高梯度, 牛顿迭代法

中图分类号：O34　　**文献标识码**：A　　doi：10.6052/0459-1879-19-005

FINTE SUBDOMAIN RADIAL BASIS COLLOCATION METHOD FOR THE LARGE DEFORMATION ANALYSIS [1)]

Wang Lihua[*,2)]　Li Yiming[*]　Chu Fuyun [†]

[*](*School of Aerospace Engineering and Applied Mechanics*，*Tongji University*，*Shanghai* 200092，*China*)

[†](*Aerospace System Engineering Shanghai*，*Shanghai* 201109，*China*)

Abstract　The meshfree methods can avoid grid distortion problems because it does not need to be meshed, which make them widely used in large deformations and other complicated problems. Radial basis collocation method (RBCM) is a typical strong form meshfree method. This method has the advantages of no need for any mesh, simple solution process, high precision, good convergence and easy expansion to high-dimensional problems. Since the global shape function is used, this method has the disadvantages of low precision and poor representation to local characteristics when solving high gradient problems. To resolve this issue, this paper introduces finite subdomain radial basis collocation method to solve the large deformation problem with local high gradients. Based on the total Lagrangian formulation, the Newton iteration method is used to establish the incremental solution scheme of the FSRBCM in large deformation analysis. This method partitions the solution domain into several subdomains according to its geometric characteristics, then constructs radial basis function interpolation in the subdomains, and imposes all the interface continuous conditions on the interfaces, which

2019–01–04 收稿, 2019–04–19 录用, 2019–04–19 网络版发表.

1) 国家自然科学基金项目 (11572229) 和中央高校基本科研业务费项目 (22120180063) 资助.

2) 王莉华, 副教授, 主要研究方向：计算力学、结构动力学. E-mail: lhwang@tongji.edu.cn

引用格式：王莉华, 李溢铭, 褚福运. 基于分区径向基函数配点法的大变形分析. 力学学报, 2019, 51(3): 743-753
Wang Lihua, Li Yiming, Chu Fuyun. Finte subdomain radial basis collocation method for the large deformation analysis. *Chinese Journal of Theoretical and Applied Mechanics*, 2019, 51(3): 743-753

results in a block sparse matrix for the numerical solution. The proposed method has super convergence and transforms the original full matrix into a sparse matrix, which reduces the storage space and improves the computational efficiency. Compared to the traditional RBCM and finite element method (FEM), this method can better reflect local characteristics and solve high gradient problems. Numerical simulations show that the method can effectively solve the large deformation problems with local high gradients.

Key words meshfree, finite subdomain radial basis collocation method, large deformation, high gradient, Newton iteration method

引 言

无网格法通过点来离散求解区域, 不需要划分网格, 因此不会发生网格畸变问题, 使得其广泛应用于大变形和一些复杂问题 [1-9]. 无网格法构建方程的模式主要包括两大类：基于 Galerkin 法的积分弱形式 [1,6,10-13] 和基于直接配点法的强形式 [14-18]. 配点型无网格法由于不需要积分, 能够获得比有限元法更高的效率 [19-21], 因此逐渐获得了更多的关注 [22], 高效配点型无网格法已广泛应用于声子晶体 [23]、优化 [24]、结构振动 [25]、环境工程 [26] 等方面. 径向基函数配点法 (radial basis collocation method, RBCM) 是一种典型的强形式无网格法, 这种方法具有完全不需要任何网格、求解过程简单、精度高、收敛性好以及易于扩展到高维空间等优点 [27-28]. 其在分析大变形问题时, 具有不存在网格畸变等优势, 但是由于其采用全域的形函数, 在求解高梯度问题时会存在精度较低和无法很好地反应局部特性的缺点 [29-30].

为有效改善传统径向基函数配点法存在的问题, 本文引入分区径向基函数配点法 (finite subdomain radial basis collocation method, FSRBCM)[31] 来求解局部存在高梯度的大变形问题. 这种方法首先将求解域根据其几何特点或材料性质等划分成若干个子 (区) 域, 在子域内构建径向基函数插值. 在界面上施加所有的界面连续条件, 在不同的子域内可以根据局域特性选用不同的形状参数, 构建统一的配点方程并一次求解. 与传统区域分解法 (domain decomposition method)[32] 不同的是, 区域分解法在子域边界上需要大量的迭代计算, 有时候还会存在不收敛的问题. 而分区配点法的界面连续条件不需要迭代求解, 计算效率高. 该方法仍然保持超收敛性, 且将原来的满阵转化成了稀疏矩阵, 降低了条件数和存储空间, 提高了计算效率. 也为求解大规模科学计算问题打下了基础.

本文从强形式控制方程出发, 基于分区径向基函数配点法建立了大变形问题的求解格式. 通过牛顿迭代法对非线性方程进行线性化, 采用完全拉格朗日格式, 得到了用于分析大变形问题的增量模式, 在每个迭代步内, 采用分区径向基函数配点法一次求解. 数值算例表明分区径向基函数配点法能够很好地反应问题的局部高梯度特性.

1 径向基函数近似

径向基函数 (radial basis function, RBF) 是一类函数值取决于计算点 $\boldsymbol{x}$ 与源点 $\boldsymbol{x}_I$ 之间距离的实值函数 [28,33]. 常见的径向基函数有 Multiquadrics(MQ) 径向基函数、高斯径向基函数和薄板样条径向基函数等. 由于 MQ 径向基函数具有较高的精度和收敛率, 本文采用 MQ 进行求解分析, 其表达式如下

$$g_I(\boldsymbol{x}) = \left(r_I^2 + c^2\right)^{\vartheta - \frac{3}{2}} \tag{1}$$

式中，$r_I = \|\boldsymbol{x} - \boldsymbol{x}_I\|_2$ 表示计算点与源点的距离, 形状参数 c 是大于 0 的常数, ϑ 的取值不同表示不同类型的 MQ 径向基函数, 本文中取 $\vartheta = 1$.

2 大变形分析

2.1 基本方程

某弹性力学问题的求解域为 $\varOmega$, Neumann 边界为 $\varGamma$, Dirichlet 边界为 $\varPi$, 边界 $\partial\varOmega = \varGamma \cup \varPi$, 区域 $\bar{\varOmega} = \varOmega \cup \partial\varOmega$. 初始构形用坐标 X 表示, 变形之后的现时构形用坐标 x 表示. 采用 Kirchhoff 应力 S 表示的初始位形空间描述的平衡方程表示如下

$$\left.\begin{aligned} &\left(S_{kj}F_{ik}\right)_{,j} + b_i = 0\,, && \text{in } \varOmega \\ &S_{jk}F_{ij}N_k = h_i && \text{on } \varGamma \\ &u_i = g_i\,, && \text{on } \varPi \end{aligned}\right\} \tag{2}$$

其中, $F_{ik} = \partial x_i/\partial X_k$ 为变形梯度, b_i 体力, h_i 是 Neumann 边界 $\varGamma$ 上的表面力, N_k 是曲面法线, g_i 是 Dirichlet 边界 Π 上的已知位移. 对于线弹性材料

$$S_{ij} = D_{ijkl}\varepsilon_{kl} \tag{3}$$

其中

$$\varepsilon_{ij} = \frac{1}{2}\left(\frac{\partial u_i}{\partial X_j} + \frac{\partial u_j}{\partial X_i} + \frac{\partial u_k}{\partial X_i}\frac{\partial u_k}{\partial X_j}\right) \tag{4}$$

式中，D_{ijkl} 为常数.

将求解区域分成 m 个互不重叠的子域 $\Omega = \Omega^1 \cup \Omega^2 \cup \cdots \cup \Omega^m$. 对于任一子域 $\alpha,\beta = 1,2,\cdots,m$, 其中 $\Omega^\alpha \cap \Omega^\beta = \emptyset\ (\alpha \neq \beta)$, $\partial\Omega^\alpha \cap \partial\Omega^\beta = \emptyset\ (\alpha \neq \beta)$, $\Lambda_{\alpha\beta} = \bar{\Omega}^\alpha \cap \bar{\Omega}^\beta$ 任一子域的控制方程可表示如下

$$\left.\begin{aligned}&\left(S^\alpha_{kj}F^\alpha_{ik}\right)_{,j} + b^\alpha_i = 0, && \text{in } \Omega^\alpha\\ &S^\alpha_{jk}F^\alpha_{ij}N^\alpha_k = h^\alpha_i, && \text{in } \Gamma^\alpha\\ &u^\alpha_i = g^\alpha_i, && \text{in } \Pi^\alpha\end{aligned}\right\} \tag{5}$$

界面连续条件为

$$\left.\begin{aligned}&S^\alpha_{jk}F^\alpha_{ij}N^\alpha_k + S^\beta_{jk}F^\beta_{ij}N^\beta_k = 0\\ &u^\alpha_i = u^\beta_i\end{aligned}\right\} \quad \text{in } \Lambda_{\alpha\beta} \tag{6}$$

2.2 近似函数

子域中的未知量可以采用该子域内的径向基函数近似表示为

$$(u^\alpha(\boldsymbol{X}))^h = \sum_{I=1}^{\xi^\alpha} g^\alpha_I(\boldsymbol{X})\, a_I, \quad X \in \bar{\Omega}^\alpha \tag{7}$$

其中，ξ^α 为 α 子域中源点的个数. 方程 (7) 可以写成如下的一般形式

$$\left(u^\alpha_i\right)^h = (\boldsymbol{\Phi}^\alpha)^{\mathrm{T}}\boldsymbol{a} \tag{8}$$

其中

$$(\boldsymbol{\Phi}^\alpha)^{\mathrm{T}} = \left[\boldsymbol{g}^\alpha_1, \boldsymbol{g}^\alpha_2, \cdots, \boldsymbol{g}^\alpha_{N^\alpha}\right], \quad \boldsymbol{g}^\alpha_I = g^\alpha_I\boldsymbol{I} \tag{9}$$

式中，g^α_I 是子域中源点 $\boldsymbol{x}_I \in \bar{\Omega}^\alpha$ 的径向基函数近似, $\boldsymbol{I}$ 是单位矩阵. 在每个子域及其边界和界面上定义如下的配点集合

$$\left.\begin{aligned}&\boldsymbol{P}^\alpha = \{\boldsymbol{p}_I\}^{\zeta^\alpha_p}_{I=1} \subseteq \Omega^\alpha, \quad \boldsymbol{Q}^\alpha = \{\boldsymbol{q}_I\}^{\zeta^\alpha_q}_{I=1} \subseteq \Gamma^\alpha\\ &\boldsymbol{R}^\alpha = \{\boldsymbol{r}_I\}^{\zeta^\alpha_r}_{I=1} \subseteq \Pi^\alpha, \quad \boldsymbol{Z}_{\alpha\beta} = \{\boldsymbol{z}_I\}^{\zeta_{\alpha\beta}}_{I=1} \subseteq \Lambda_{\alpha\beta}\end{aligned}\right\} \tag{10}$$

其中，ζ^α_p，ζ^α_q，ζ^α_r，$\zeta_{\alpha\beta}$ 分别表示 α 子域中域内、Neumann 边界、Dirichlet 边界和与 α 子域相邻界面上的配点个数. 通常情况下, 子域内选取的配点个数大于源点个数.

2.3 大变形问题求解

根据牛顿迭代原理, 其增量迭代格式可以表示为

$$\left.\begin{aligned}&\Delta\left[\left(S^\alpha_{kj}F^\alpha_{ik}\right)_{,j} + b^\alpha_i\right]^n_{v+1} = -\left[\left(S^\alpha_{kj}F^\alpha_{ik}\right)_{,j} + b^\alpha_i\right]^n_v, && \text{in } \Omega^\alpha\\ &\Delta\left(S^\alpha_{kj}F^\alpha_{ik}N^\alpha_j\right)^n_{v+1} = \left(h^\alpha_i\right)^n - \left(S^\alpha_{kj}F^\alpha_{ik}N^\alpha_j\right)^n_v, && \text{in } \Gamma^\alpha\\ &\Delta\left(u^\alpha_i\right)^n_{v+1} = \left(g^\alpha_i\right)^n - \left(u^\alpha_i\right)^n_v, && \text{in } \Pi^\alpha\end{aligned}\right\} \tag{11}$$

其中 n 和 v 分别表示载荷步和迭代步. 在第 n 载荷步上进一步展开得到

$$\begin{aligned}&\left(F^\alpha_{ik,j}\right)_v\left(\Delta S^\alpha_{kj}\right)_{v+1} + \left(S^\alpha_{kj}\right)_v\left(\Delta F^\alpha_{ik,j}\right)_{v+1} +\\ &\quad\left(F^\alpha_{ik}\right)_v\left(\Delta S^\alpha_{kj,j}\right)_{v+1} + \left(S^\alpha_{kj,j}\right)_v\left(\Delta F^\alpha_{ik}\right)_{v+1} =\\ &\quad b^\alpha_i - \left(F^\alpha_{ik,j}S^\alpha_{kj} + F^\alpha_{ik}S^\alpha_{kj,j}\right)_v, \quad \text{in } \Omega^\alpha\end{aligned} \tag{12}$$

$$\begin{aligned}&\left(S^\alpha_{kj}N^\alpha_k\right)_v\left(\Delta F^\alpha_{ik}\right)_{v+1} + \left(F^\alpha_{ik}N^\alpha_j\right)_v\left(\Delta S^\alpha_{kj}\right)_{v+1} =\\ &\quad h^\alpha_i - \left(S^\alpha_{kj}F^\alpha_{ik}N^\alpha_j\right)_v, \quad \text{in } \Gamma^\alpha\end{aligned} \tag{13}$$

$$\left(\Delta u^\alpha_i\right)_{v+1} = g^\alpha_i - \left(u^\alpha_i\right)_v, \quad \text{in } \Pi^\alpha \tag{14}$$

对于相邻公共边界上的连续条件式 (6), 也可以利用牛顿迭代法得到如下的增量迭代格式

$$\begin{aligned}&\left(S^\alpha_{kj}N^\alpha_j\right)_v\left(\Delta F^\alpha_{ik}\right)_{v+1} + \left(F^\alpha_{ik}N^\alpha_j\right)_v\left(\Delta S^\alpha_{kj}\right)_{v+1} +\\ &\quad\left(S^\beta_{kj}N^\beta_j\right)_v\left(\Delta F^\beta_{ik}\right)_{v+1} + \left(F^\beta_{ik}N^\beta_j\right)_v\left(\Delta S^\beta_{kj}\right)_{v+1} =\\ &\quad -\left(S^\alpha_{kj}F^\alpha_{ik}N^\alpha_j\right)_v - \left(S^\beta_{kj}F^\beta_{ik}N^\beta_j\right)_v, \quad \text{in } \Lambda_{\alpha\beta}\end{aligned} \tag{15}$$

$$\left(\Delta u^\alpha_i\right)_{v+1} - \left(\Delta u^\beta_i\right)_{v+1} = \left(u^\beta_i\right)_v - \left(u^\alpha_i\right)_v, \quad \text{in } \Lambda_{\alpha\beta} \tag{16}$$

将径向基函数近似式 (7) 代入增量方程 (12) ~ (16), 即可得到在所有子域 Ω、边界 $\partial\Omega$ 和相邻界面 Λ 上增量迭代格式的离散形式, 用矩阵表示为

$$\boldsymbol{K}\Delta\boldsymbol{a} = \boldsymbol{f} \tag{17}$$

其中矩阵定义为

$$\boldsymbol{K} = \begin{bmatrix}\boldsymbol{K}^1\\ \boldsymbol{K}^2\\ \vdots\\ \boldsymbol{K}^m\end{bmatrix}, \ \boldsymbol{K}^\alpha = \begin{bmatrix}\boldsymbol{K}^\alpha_L\\ \boldsymbol{K}^\alpha_h\\ \boldsymbol{K}^\alpha_g\\ \boldsymbol{K}^\alpha_{\Lambda_h}\\ \boldsymbol{K}^\alpha_{\Lambda_g}\end{bmatrix}, \ \boldsymbol{f} = \begin{bmatrix}\boldsymbol{f}^1\\ \boldsymbol{f}^2\\ \vdots\\ \boldsymbol{f}^m\end{bmatrix}, \ \boldsymbol{f}^\alpha = \begin{bmatrix}\boldsymbol{f}^\alpha_L\\ \boldsymbol{f}^\alpha_h\\ \boldsymbol{f}^\alpha_g\\ \boldsymbol{f}^\alpha_{\Lambda_h}\\ \boldsymbol{f}^\alpha_{\Lambda_g}\end{bmatrix} \tag{18}$$

$$\begin{aligned}\boldsymbol{K}^\alpha_L = \boldsymbol{K}^\alpha_L = &\ \boldsymbol{L}\boldsymbol{D}_1\boldsymbol{B}_1 + (\boldsymbol{L}_2\boldsymbol{D}_2\boldsymbol{A}_3 + \boldsymbol{S}_1)\,\boldsymbol{B}_2 +\\ &(\boldsymbol{L}\boldsymbol{D}_1\boldsymbol{A}_1 + \boldsymbol{L}_2\boldsymbol{D}_2\boldsymbol{A}_2 + \boldsymbol{T}_1 + \boldsymbol{T}_2)\,\boldsymbol{B}_3\end{aligned} \tag{19}$$

$$\boldsymbol{K}_h^\alpha = \boldsymbol{K}_{\Lambda_h}^\alpha = \boldsymbol{L}_2\boldsymbol{N}_1\boldsymbol{D}_1(\boldsymbol{B}_1 + \boldsymbol{A}_1\boldsymbol{B}_3) + \boldsymbol{N}_2\boldsymbol{S}_2\boldsymbol{B}_3 \tag{20}$$

$$\boldsymbol{K}_g^\alpha = \boldsymbol{K}_{\Lambda_g}^\alpha = \begin{bmatrix} (\boldsymbol{\Phi}^\alpha)^{\mathrm{T}} & \boldsymbol{0} \\ \boldsymbol{0} & (\boldsymbol{\Phi}^\alpha)^{\mathrm{T}} \end{bmatrix} \tag{21}$$

$$\boldsymbol{f}_L^\alpha = \boldsymbol{b} - \boldsymbol{L}\boldsymbol{S} - \boldsymbol{L}_2(\boldsymbol{T}_3 + \boldsymbol{T}_4) \tag{22}$$

$$\boldsymbol{f}_h^\alpha = \boldsymbol{h} - \boldsymbol{N}_2\boldsymbol{L}_3\boldsymbol{S} \tag{23}$$

$$\boldsymbol{f}_g^\alpha = \boldsymbol{g} - \boldsymbol{u} \tag{24}$$

$$\boldsymbol{f}_{\Lambda_h}^\alpha = \boldsymbol{f}_{\Lambda_g}^\alpha = \boldsymbol{0} \tag{25}$$

在矩阵 $\boldsymbol{f}_L^\alpha$ 和 $\boldsymbol{f}_L^\alpha$ 中 $\boldsymbol{\Phi}^\alpha = \boldsymbol{\Phi}^\alpha(\boldsymbol{p}^\alpha)$, 矩阵 $\boldsymbol{K}_h^\alpha$ 和 $\boldsymbol{f}_h^\alpha$ 中 $\boldsymbol{\Phi}^\alpha = \boldsymbol{\Phi}^\alpha(\boldsymbol{q}^\alpha)$, 矩阵 $\boldsymbol{K}_g^\alpha$ 和 $\boldsymbol{f}_g^\alpha$ 中 $\boldsymbol{\Phi}^\alpha = \boldsymbol{\Phi}^\alpha(\boldsymbol{r}^\alpha)$, 矩阵 $\boldsymbol{K}_{\Lambda_h}^\alpha$ 和 $\boldsymbol{K}_{\Lambda_g}^\alpha$ 中 $\boldsymbol{\Phi}^\alpha = \boldsymbol{\Phi}^\alpha(\boldsymbol{z}^\alpha)$. 方程 (19)~(23) 各矩阵的详细表达式见附录.

由于子域内部、边界以及界面上的误差由于计算数据大小的差异在数值计算中会出现不平衡的问题, 在边界和界面上需施加合适的权重以获得最优的精度和收敛率 [31]. 方程 (17) 的加权形式表示如下

$$\boldsymbol{W}\boldsymbol{K}\Delta\boldsymbol{a} = \boldsymbol{W}\boldsymbol{f} \tag{26}$$

$$\boldsymbol{W} = \begin{bmatrix} \boldsymbol{W}^1 \\ \boldsymbol{W}^2 \\ \vdots \\ \boldsymbol{W}^m \end{bmatrix}, \quad \boldsymbol{W}^\alpha = \begin{bmatrix} \boldsymbol{1} \\ \boldsymbol{W}_h^\alpha \\ \boldsymbol{W}_g^\alpha \\ \boldsymbol{W}_{\Lambda_h}^\alpha \\ \boldsymbol{W}_{\Lambda_g}^\alpha \end{bmatrix} \tag{27}$$

其中应力边界和位移边界的权重取值如下

$$\left.\begin{aligned} & w_h^\alpha \approx O(\theta^\alpha), \ w_g^\alpha \approx O(\kappa^\alpha \xi^\alpha) \\ & w_{\Lambda_h}^{\alpha\beta} \approx O(1), \ w_{\Lambda_g}^{\alpha\beta} \approx O\left(\kappa^{\alpha\beta}\xi^{\alpha\beta}\right) \end{aligned}\right\} \tag{28}$$

其中，$\kappa^\alpha = \max(\lambda^\alpha, \mu^\alpha)$, $\kappa^{\alpha\beta} = \max(\kappa^\alpha, \kappa^\beta)$, $\theta^\alpha = \kappa^{\alpha\beta}/\kappa^\alpha$, $\xi^{\alpha\beta} = \max(\xi^\alpha, \xi^\beta)$, ξ^α 和 ξ^β 即对应 α 和 β 两个子域内选取的源点数目, λ^α 和 μ^α 为 α 子域中材料的拉梅常数. 超定方程 (27) 通常可以采用最小二乘法、截断奇异值分解法等方法进行求解.

2.4 程序设计

对于弹性大变形问题, 受到静力载荷作用, 基于完全拉格朗日格式 (total Lagrangian), 具体的程序设计和求解步骤如下：

(1) 确定初始构型, 区域划分模式, 子域个数以及域内、边界和界面上的源点和配点分布, 设置载荷增量.

(2) 在第一个载荷步中 (在第 n 个载荷步中), 取第一个迭代步的初始近似值 $\boldsymbol{a}_0$.

(3) 计算得到 $\boldsymbol{u}_0 = \boldsymbol{\Phi}\boldsymbol{a}_0(\boldsymbol{u}_v = \boldsymbol{\Phi}\boldsymbol{a}_v)$. 根据式 (19) ~ 式 (25) 和 $\boldsymbol{u}_0$ $(\boldsymbol{u}_v)$ 计算出每个子域上的 $\boldsymbol{K}_L$, $\boldsymbol{K}_h$, $\boldsymbol{K}_g$, $\boldsymbol{K}_{\Lambda_h}$, $\boldsymbol{K}_{\Lambda_g}$, $\boldsymbol{f}_L$, $\boldsymbol{f}_h$, $\boldsymbol{f}_g$, $\boldsymbol{f}_{\Lambda_h}$, $\boldsymbol{f}_{\Lambda_h}$, 组装成整体矩阵 $\boldsymbol{K}$ 和 $\boldsymbol{f}$, 通过方程 (17) 求出增量 $\Delta\boldsymbol{a}_1$ $(\Delta\boldsymbol{a}_v)$.

(4) 判断 $\Delta\boldsymbol{u}_1 = \boldsymbol{\Phi}\Delta\boldsymbol{a}_1$ $(\Delta\boldsymbol{u}_v = \boldsymbol{\Phi}\Delta\boldsymbol{a}_v)$ 是否满足下式

$$\|\Delta\boldsymbol{u}\| \leqslant e \tag{29}$$

其中，e 为人工设置的误差界限. 如果满足, 则进入式 (5). 如果不满足, 取新的近似值为

$$\boldsymbol{a}_1 = \boldsymbol{a}_0 + \Delta\boldsymbol{a}_1 \ \ (\boldsymbol{a}_{v+1} = \boldsymbol{a}_v + \Delta\boldsymbol{a}_{v+1}) \tag{30}$$

然后返回式 (3) 继续迭代求解.

(5) 在载荷中增加载荷增量进入下一个分析步. 然后依据式 (2) ~ 式 (4) 的过程循环求解, 直至载荷步全部计算结束.

3 数值算例

3.1 受均布载荷作用的悬臂梁

如图 1 所示, 悬臂梁在上下表面受到均布载荷作用, 材料参数为：弹性模量 $E = 12\,\mathrm{kPa}$, 泊松比 $\nu = 0.2$. 梁的长度和宽度分别为 $L = 10\,\mathrm{m}$, $H = 1\,\mathrm{m}$. 载荷为 $q = 5\,\mathrm{N/m}$, 载荷步为 150 步. 总源点个数 $\xi = 9 \times 51$, 源点分布如图 2 所示, 在分区径向基函数配点法中将整体区域划分成 2 个子域. 边界和界面上所取的权重为：$w_h^\alpha = 10$, $w_g^\alpha = 1 \times 10^3$, $w_{\Lambda_h}^{\alpha\beta} = 100$, $w_{\Lambda_g}^{\alpha\beta} = 1 \times 10^4$ $(\alpha = 1, 2;\ \beta = 1, 2)$. 梁端挠度、横向位移随载荷的变化和柯西应力如图 3 和图 4 所示 (位移解析解参见文献 [34]), 结果表明, 对于局部存在高梯度的问题, 分区径向基函数配点法能比径向基函数配点法获得更高的精度；有限元法求解的位移精度较低, 而且在局部高梯度区域会出现应力波动. 图 5 所示的挠度和横向位移收敛图表明分区径向基函数配点法在求解这类问题时仍能获得高收敛率. 由于分区后形成了稀疏矩阵, 如图 6 所示, 分区径向基函数配点法会比径向基函数配点法节约大约一半的计算时间, 显著地提高了计算效率.

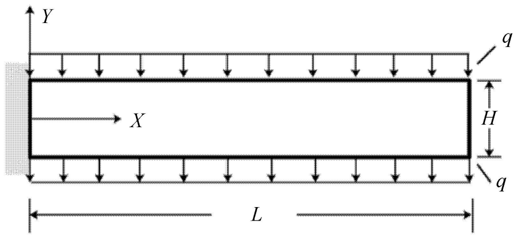

图 1 受均布载荷作用的悬臂梁

Fig. 1 Cantivilever beam under uniform load

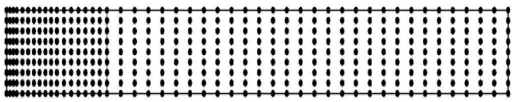

图 2 悬臂梁源点分布图

Fig. 2 Distribution of source points for cantivilever beam

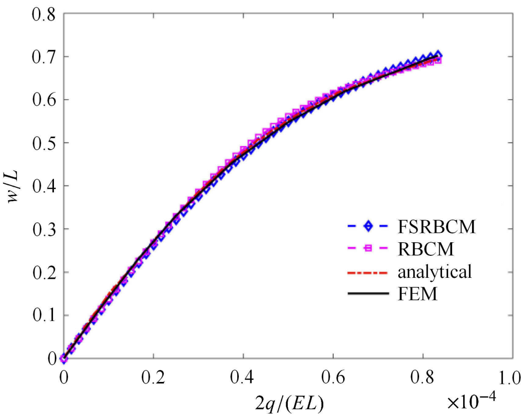

(a) 挠度

(a) Deflection

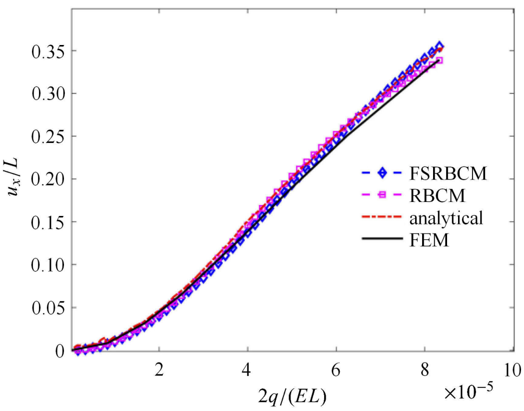

(b) 横向位移

(b) Lateral displacement

图 3 悬臂梁梁端挠度、横向位移和载荷的关系图

Fig. 3 Deflection and lateral displacement of the end point of cantilever beam

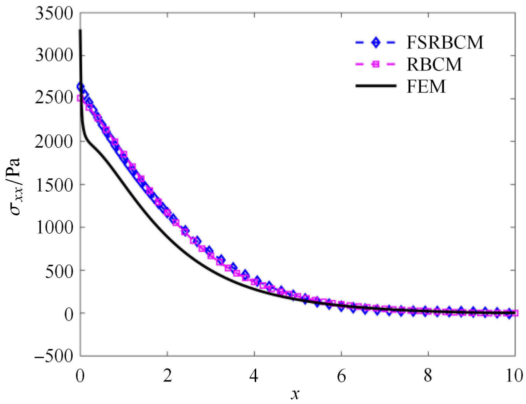

图 4 悬臂梁上表面的柯西应力图

Fig. 4 Cauchy stress on the upper surface of cantilever beam

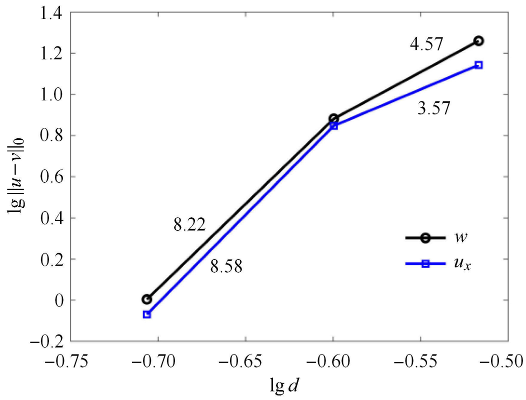

图 5 悬臂梁挠度和横向位移收敛图

Fig. 5 Convergence of the deflection and lateral displacement for cantilever beam

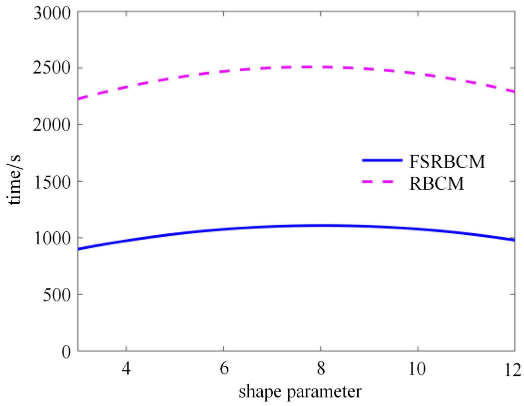

图 6 悬臂梁计算时间对比

Fig. 6 Comparison of the CPU time for cantilever beam

3.2 纯弯曲悬臂梁

在右端部受纯弯曲载荷作用的悬臂梁如图 7 所示, 材料参数为：$E = 210\,\text{GPa}$, $\nu = 0.3$, 梁的尺寸为：长 $L = 3\,\text{m}$, 宽 $H = 0.3\,\text{m}$. 载荷为 $M = 0.15\,\text{GN·m}$, 载荷步为 150 步. 源点分布如图 8 所示, 源点个数

为 $\xi = 9\times45$, 在分区径向基函数配点法中整体区域划分成了 3 个子域. 施加在边界和界面上的权重为：$w_h^\alpha = 10$, $w_g^\alpha = 2\times10^{10}$, $w_{\Lambda_h}^{\alpha\beta} = 10$, $w_{\Lambda_g}^{\alpha\beta} = 2\times10^{10}$ ($\alpha = 1,2,3$; $\beta = 1,2,3$). 图 9 和图 10 中的挠度、横

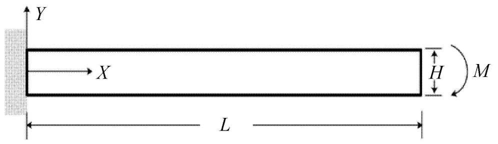

图 7 纯弯曲作用下的悬臂梁

Fig. 7 Cantivilever beam under bending

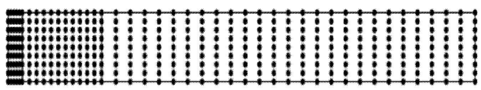

图 8 纯弯曲梁源点分布图

Fig. 8 Distribution of source points for pure bending beam

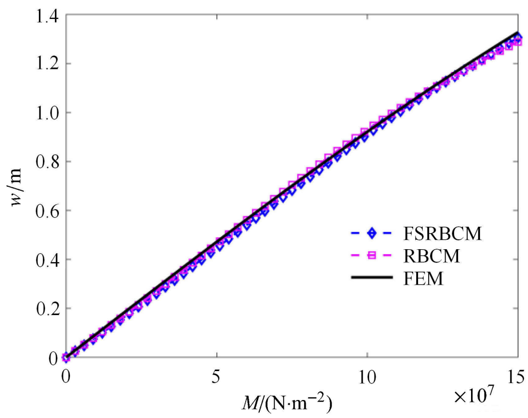

(a) 挠度

(a) Deflection

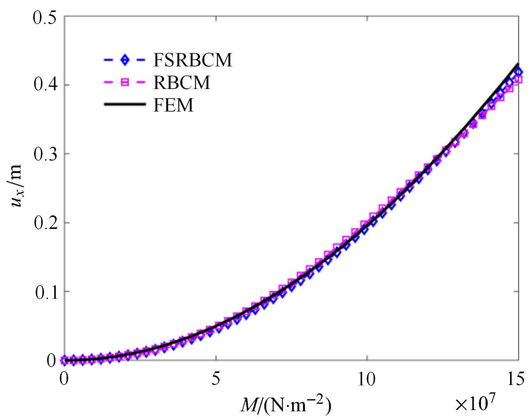

(b) 横向位移

(b) Lateral displacement

图 9 纯弯曲梁端挠度、横向位移和载荷的关系图

Fig. 9 Deflection and lateral displacement of the end point of pure bending beam

向位移和柯西应力分布再次表明分区径向基函数配点法在求解局部高梯度问题中具有优势, 传统径向基函数配点法的求解精度较低, 而有限元法在求解应力时容易在局部高梯度区域出现应力波动. 图 11 表明在求解这类问题时分区径向基函数配点法能够显著提高计算效率.

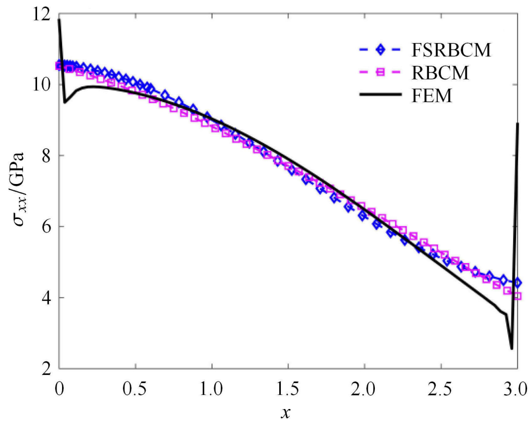

图 10 纯弯曲梁上表面的柯西应力图

Fig. 10 Cauchy stress on the upper surface of pure bending beam

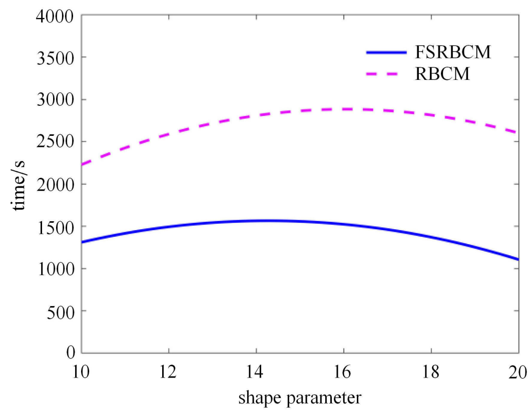

图 11 纯弯曲梁计算时间对比

Fig. 11 Comparison of CPU time for pure bending beam

3.3 拉伸作用下的带孔板

受拉伸作用的正方形板中央带圆孔如下图 12 所示, $a = 1$ m, 右侧受拉伸均布荷载 $q = 1$ N/m, 材料参数为：$E = 1\times10^3$ Pa, $\nu = 0.3$. 取 1/4 进行分析, 源点个数 $\xi = 25\times25$, 源点分布如图 13 所示, 将区域划分为 4 个子域, 取载荷步为 200 步. 边界和界面上的权重为：$w_h^\alpha = 10$, $w_g^\alpha = 1\times10^3$, $w_{\Lambda_h}^{\alpha\beta} = 100$, $w_{\Lambda_g}^{\alpha\beta} = 1\times10^4$ ($\alpha = 1,2,3,4$; $\beta = 1,2,3,4$). 左侧简支边界的 y 方向的位移结果分布图和下侧简支边界 x 方向的位移结果分布图如图 14 所示. 图 15 给出了左侧简支边

界和下侧简支边界上 x 方向的应力分布. 结果表明, 分区径向基函数配点法能够比径向基函数配点法获得更好的精度 (以稠密单元的有限元解作为参考解). 相对于受均布载荷作用和纯弯曲作用的悬臂梁算例, 带孔板的局部梯度变化较小, 所以有限元法也获得了比较好的数值结果, 没有出现明显的应力波动. 图 16 表明相比于全域的径向基函数配点法, 分区形式能够显著提高计算效率.

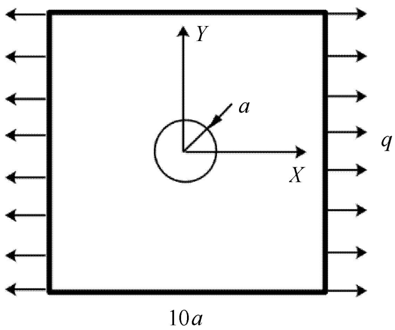

图 12 受拉伸作用的带孔板

Fig. 12 Plate with hole under tension

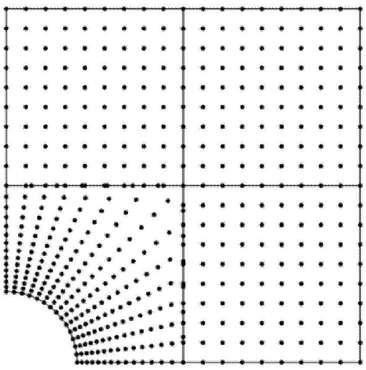

图 13 带孔板源点分布图

Fig. 13 Distribution of source points for plate with hole

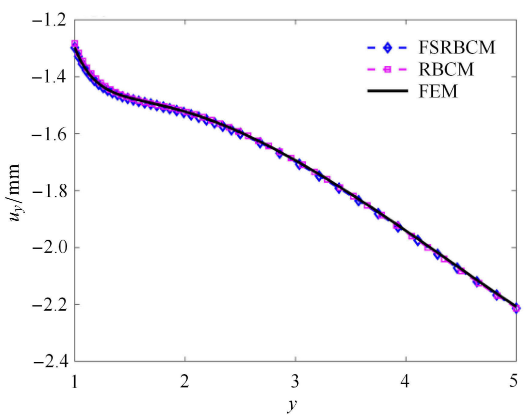

(a) 左侧简支边

(a) Left edge

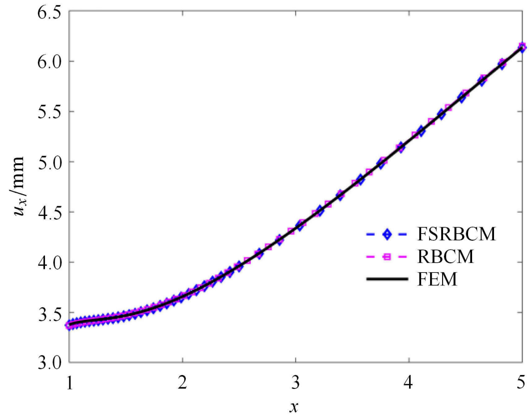

(b) 下侧简支边

(b) Underside edge

图 14 带孔板边界位移分布

Fig. 14 Displacement of the simply supported boundary of plate with hole

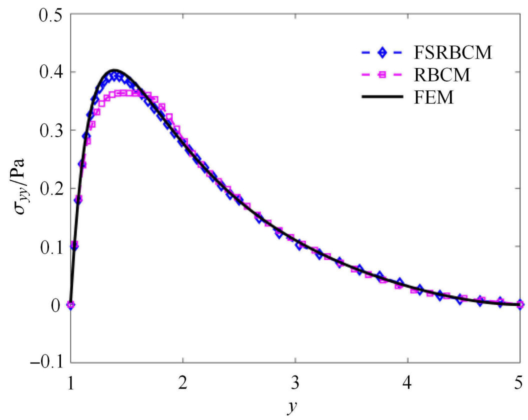

(a) 左侧简支边

(a) Left edge

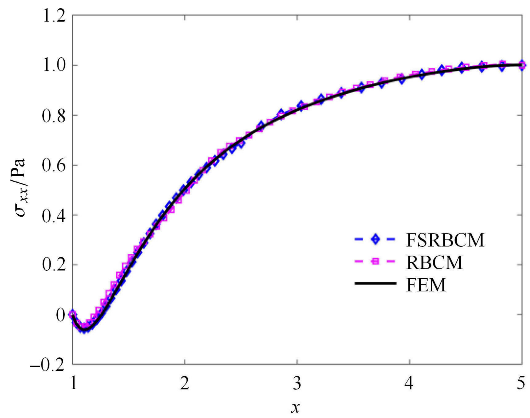

(b) 下侧简支边

(b) Underside edge

图 15 带孔板边界应力分布

Fig. 15 Cauchy stress of the simply supported boundary of plate with hole

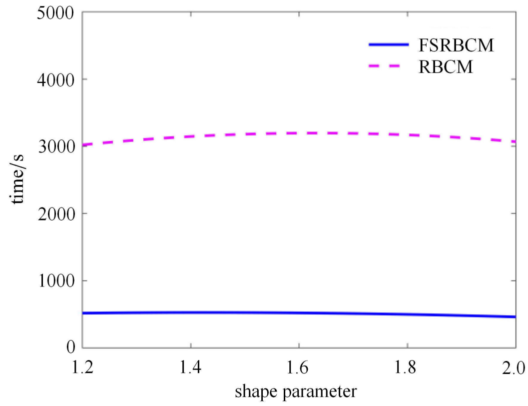

图 16 带孔板计算时间对比

Fig. 16 Comparison of CPU time for plate with hole

4 结 论

由于传统径向基函数配点法在求解高梯度问题时往往会存在精度低和收敛率低的问题, 本文引入分区径向基函数配点法求解了局部存在高梯度的弹性大变形问题. 基于完全拉格朗日格式和牛顿迭代原理, 建立了弹性大变形问题分区配点模式的增量迭代格式. 数值分析表明, 相比较于传统径向基函数配点法, 分区径向基函数配点法在求解高梯度大变形问题中不仅能够获得较高的精度和收敛率, 而且能够显著提高计算效率. 相比较于有限元法, 其得到的应力数值结果比较光滑, 能够避免传统有限元法在求解高梯度问题时出现的应力波动问题. 因此, 分区径向基函数配点法在求解复杂的大变形问题中具有较好的应用前景.

参 考 文 献

1 Belytschko T, Lu YY, Gu L. Element-free galerkin methods. *International Journal for Numerical Methods in Engineering*, 1994, 37(2): 229-256

2 Belytschko T, Krongauz Y, Organ D, et al. Meshless methods: an overview and recent developments. *Computer Methods in Applied Mechanics and Engineering*, 1996, 139(1-4): 3-47

3 Liu WK, Jun S, Zhang YF. Reproducing kernel particle methods. *International Journal for Numerical Methods in Fluids*, 1995, 20(8-9): 1081-1106

4 张雄, 刘岩, 马上. 无网格法的理论及应用. 力学进展, 2009, 39(1): 1-36 (Zhang Xiong, Liu Yan, Ma Shang. Meshfree method and their applications. *Advance in Mechanics*, 2009, 39(1): 1-36 (in Chinese))

5 Chen JS, Hillman M, Chi SW. Meshfree methods: Progress made after 20 years. *Journal of Engineering Mechanics*, 2017, 143(4): 04017001

6 Chen JS, Pan C, Wu CT, et al. Reproducing kernel particle methods for large deformation analysis of non-linear structures. *Computer Methods in Applied Mechanics and Engineering*, 1996, 139(1-4): 195-227

7 程玉民, 李九红. 弹性力学的复变量无网格方法. 物理学报, 2005, 54(10): 4463-4471 (Chen Yuming, Li Jiuhong. A meshless method with complex variables for elasticity. *Acta Physica Sinica*, 2005, 54(10): 4463-4471 (in Chinese))

8 Liu MB, Liu GR. Smoothed particle hydrodynamics (SPH): An overview and recent developments. *Archives of Computational Methods in Engineering*, 2010, 17(1): 25-76

9 邓立克, 王东东, 王家睿等. 薄板分析的线性基梯度光滑伽辽金无网格法. 力学学报, 2019, 51(3) (Deng Like, Wang Dongdong, Wang Jiarui, et al. A gradient smoothing Galerkin meshfree method for thin plate analysis with linear basis function. *Chinese Journal of Theoretical and Applied Mechanics*, 2019, 51(3) (in Chinese))

10 Chen J, Wu C, Yoon S. A stabilized conforming nodal integration for Galerkin mesh-free methods. *International Journal for Numerical Methods in Engineering*, 2001, 50(2): 435-466

11 Wang D, Chen JS. Locking-free stabilized conforming nodal integration for meshfree Mindlin-Reissner plate formulation. *Computer Methods in Applied Mechanics and Engineering*, 2004, 193(12-14): 1065-1083

12 宋彦琦, 周涛. 基于 S-R 和分解定理的三维几何非线性无网格法. 力学学报, 2018, 50(4): 853-862 (Song Yanqi, Zhou Tao. Three-dimensional geometric nonlinearity element-free method based on S-R decomposition theorem. *Chinese Journal of Theoretical and Applied Mechanics*, 2018, 50(4): 853-862 (in Chinese))

13 马文涛. 二维弹性力学问题的光滑无网格伽辽金法. 力学学报, 2018, 50(5): 147-156 (Ma Wentao. A smoothed meshfree galerkin method for 2d elasticity problem. *Chinese Journal of Theoretical and Applied Mechanics*, 2018, 50(5): 1115-1124(in Chinese))

14 Zhang X, Song KZ, Lu MW, et al. Meshless methods based on collocation with radial basis functions. *Computational Mechanics*, 2000, 26(4): 333-343

15 Aluru NR. A point collocation method based on reproducing kernel approximations. *International Journal for Numerical Methods in Engineering*, 2015, 47(6): 1083-1121

16 Hu HY, Chen JS, Hu W. Weighted radial basis collocation method for boundary value problems. *International Journal for Numerical Methods in Engineering*, 2010, 69(13): 2736-2757

17 Wang L, Wang Z, Qian Z. A meshfree method for inverse wave propagation using collocation and radial basis functions. *Computer Methods in Applied Mechanics & Engineering*, 2017, 322: 311-350

18 王莉华, 仲政. 基于径向基函数配点法的梁板弯曲问题分析. 固体力学学报, 2012, 33(4): 349-357 (Wang Lihua, Zhong Zheng. Radial basis collocation method for bending problems of beam and plate. *Chinese Journal of Solid Mechanics*, 2012, 33(4): 349-357 (in Chinese))

19 Li J, Chen CS, Cheng AHD. A comparison of efficiency and error convergence of multiquadric collocation method and finite element method. *Engineering Analysis with Boundry Elements*, 2003, 27(3): 251-257

20 Wang D, Wang J, Wu J. Superconvergent gradient smoothing meshfree collocation method. *Computer Methods in Applied Mechanics and Engineering*, 2018, 340: 728-766

21 Gao XW, Gao LF, Zhang Y, et al. Free element collocation method: A new method combining advantages of finite element and mesh free methods. *Computers* & *Structures*, 2019, 215: 10-26

22 Chen JS, Hillman M, Chi SW. Meshfree methods: Progress made after 20 years. *Journal of Engineering Mechanics*, 2017, 143(4): 04017001

23 Zheng H, Zhang C, Wang Y, et al. A meshfree local RBF collocation method for anti-plane transverse elastic wave propagation analysis in 2D phononic crystals. *Journal of Computational Physics*, 2016, 305: 997-1014

24 Thomas A, Majumdar P, Eldho TI, et al. Simulation optimization model for aquifer parameter estimation using coupled meshfree point collocation method and cat swarm optimization. *Engineering Analysis with Boundary Elements*, 2018, 91: 60-72

25 Qi D, Wang D, Deng L, et al. Reproducing kernel mesh-free collocation analysis of structural vibrations. *Engineering Computations*, 2019, https://doi. org/10. 1108/EC-10-2018-0439

26 Singh LG, Eldho TI, Kumar AV. Coupled groundwater flow and contaminant transport simulation in a confined aquifer using meshfree radial point collocation method (RPCM). *Engineering Analysis with Boundary Elements*, 2016, 66: 20-33

27 Kansa EJ. Multiquadrics-A scattered data approximation scheme with applications to computational fluid-dynamics-II solutions to parabolic, hyperbolic and elliptic partial differential equations. *Computers* & *Mathematics with Applications*, 1990, 19(8-9): 147-161

28 Wang L. Radial basis functions methods for boundary value problems: Performance comparison. *Engineering Analysis with Boundary Elements*, 2017, 84: 191-205

29 Chen JS, Wang L, Hu HY, et al. Subdomain radial basis collocation method for heterogeneous media. *International Journal for Numerical Methods in Engineering*, 2010, 80(2): 163-190

30 Wang L, Chen JS, Hu HY. Subdomain radial basis collocation method for fracture mechanics. *International Journal for Numerical Methods in Engineering*, 2010, 83(7): 851-876

31 Chu F, Wang L, Zhong Z. Finite subdomain radial basis collocation method. *Computational Mechanics*, 2014, 54(2): 235-254

32 Wong ASM, Hon YC, Li TS, et al. Multizone decomposition for simulation of time-dependent problems using the multiquadric scheme. *Computers* & *Mathematics with Applications*, 1999, 37(8): 23-43

33 吴宗敏．函数的径向基表示．数学进展, 1998(3): 202-208 (Wu Zongmin. Radial basis functions-a survey. *Advance in Mathematics*, 1998(3): 202-208 (in Chinese))

34 Holden JT. On the finite deflections of thin beams. *International Journal of Solids* & *Structures*, 1972, 8(8): 1051-1055

附录

式 (19) ~ 式 (23) 中的矩阵表达式如下

$$\left.\begin{aligned} \boldsymbol{L}(\boldsymbol{u}) &= \begin{bmatrix} u_1 & 0 \\ 0 & u_2 \end{bmatrix} \begin{bmatrix} \dfrac{\partial^2}{\partial X_1^2} & \dfrac{\partial^2}{\partial X_2^2} & 2\dfrac{\partial^2}{\partial X_1 \partial X_2} \\ \dfrac{\partial}{\partial X_1^2} & \dfrac{\partial^2}{\partial X_2^2} & 2\dfrac{\partial^2}{\partial X_1 \partial X_2} \end{bmatrix} \\ \boldsymbol{L}_2(\boldsymbol{u}) &= \begin{bmatrix} 1 & 0 \\ 0 & 1 \end{bmatrix} + \begin{pmatrix} u_1 & 0 \\ 0 & u_2 \end{pmatrix} \begin{pmatrix} \dfrac{\partial}{\partial X_1} & \dfrac{\partial}{\partial X_2} \\ \dfrac{\partial}{\partial X_1} & \dfrac{\partial}{\partial X_2} \end{pmatrix} \end{aligned}\right\} \tag{A1}$$

$$\boldsymbol{L}_3 = \begin{bmatrix} 1 & 0 & 0 \\ 0 & 1 & 0 \\ 0 & 0 & 1 \\ 0 & 0 & 1 \end{bmatrix} + \begin{pmatrix} u_1 & & & \\ & u_2 & & \\ & & u_1 & \\ & & & u_2 \end{pmatrix} \begin{bmatrix} \dfrac{\partial}{\partial X_1} & 0 & \dfrac{\partial}{\partial X_2} \\ 0 & \dfrac{\partial}{\partial X_2} & \dfrac{\partial}{\partial X_1} \\ 0 & \dfrac{\partial}{\partial X_2} & \dfrac{\partial}{\partial X_1} \\ \dfrac{\partial}{\partial X_1} & 0 & \dfrac{\partial}{\partial X_2} \end{bmatrix} \tag{A2}$$

$$\boldsymbol{A}_1(\boldsymbol{u}) = \begin{pmatrix} \dfrac{\partial}{\partial X_1} & \dfrac{\partial}{\partial X_1} & 0 & 0 \\ 0 & 0 & \dfrac{\partial}{\partial X_2} & \dfrac{\partial}{\partial X_2} \\ \dfrac{\partial}{\partial X_2} & \dfrac{\partial}{\partial X_2} & \dfrac{\partial}{\partial X_1} & \dfrac{\partial}{\partial X_1} \end{pmatrix} \begin{pmatrix} u_1 & & & \\ & u_2 & & \\ & & u_1 & \\ & & & u_2 \end{pmatrix} \tag{A3}$$

$$\boldsymbol{A}_2(\boldsymbol{u}) = \begin{bmatrix} \dfrac{\partial^2}{\partial X_1^2} & \dfrac{\partial^2}{\partial X_1^2} & 0 & 0 \\ 0 & 0 & \dfrac{\partial^2}{\partial X_1 \partial X_2} & \dfrac{\partial^2}{\partial X_1 \partial X_2} \\ \dfrac{\partial^2}{\partial X_1 \partial X_2} & \dfrac{\partial^2}{\partial X_1 \partial X_2} & \dfrac{\partial_1^2}{\partial X_1^2} & \dfrac{\partial^2}{\partial X_1^2} \\ \dfrac{\partial^2}{\partial X_1 \partial X_2} & \dfrac{\partial^2}{\partial X_1 \partial X_2} & 0 & 0 \\ 0 & 0 & \dfrac{\partial^2}{\partial X_2^2} & \dfrac{\partial^2}{\partial X_2^2} \\ \dfrac{\partial^2}{\partial X_2^2} & \dfrac{\partial^2}{\partial X_2^2} & \dfrac{\partial^2}{\partial X_1 \partial X_2} & \dfrac{\partial^2}{\partial X_1 \partial X_2} \end{bmatrix} \cdot \begin{pmatrix} u_1 & & & \\ & u_2 & & \\ & & u_1 & \\ & & & u_2 \end{pmatrix} \tag{A4}$$

$$\boldsymbol{A}_3(\boldsymbol{u})=\begin{bmatrix}1&0&0&0&0&0\\0&0&0&1&0&0\\0&1&1&0&0&0\\0&0&1&0&0&0\\0&0&0&0&0&1\\0&0&0&1&1&0\end{bmatrix}+\begin{bmatrix}\dfrac{\partial}{\partial X_1}&\dfrac{\partial}{\partial X_1}&0&0&0&0\\0&0&\dfrac{\partial}{\partial X_2}&\dfrac{\partial}{\partial X_2}&0&0\\\dfrac{\partial}{\partial X_2}&\dfrac{\partial}{\partial X_2}&\dfrac{\partial}{\partial X_1}&\dfrac{\partial}{\partial X_1}&0&0\\0&0&\dfrac{\partial}{\partial X_1}&\dfrac{\partial}{\partial X_1}&0&0\\0&0&0&0&\dfrac{\partial}{\partial X_2}&\dfrac{\partial}{\partial X_2}\\0&0&\dfrac{\partial}{\partial X_2}&\dfrac{\partial}{\partial X_2}&\dfrac{\partial}{\partial X_1}&\dfrac{\partial}{\partial X_1}\end{bmatrix}\begin{bmatrix}u_1&&&&&\\&u_2&&&&\\&&u_1&&&\\&&&u_2&&\\&&&&u_1&\\&&&&&u_2\end{bmatrix}\tag{A5}$$

$$\boldsymbol{B}_1=\begin{pmatrix}\dfrac{\partial}{\partial X_1}&0\\0&\dfrac{\partial}{\partial X_2}\\\dfrac{\partial}{\partial X_2}&\dfrac{\partial}{\partial X_1}\end{pmatrix}\begin{bmatrix}(\boldsymbol{\varPhi}^{\alpha})^{\mathrm{T}}&\boldsymbol{0}\\\boldsymbol{0}&(\boldsymbol{\varPhi}^{\alpha})^{\mathrm{T}}\end{bmatrix},\quad \boldsymbol{B}_3=\begin{pmatrix}\dfrac{\partial}{\partial X_1}&0\\0&\dfrac{\partial}{\partial X_1}\\\dfrac{\partial}{\partial X_2}&0\\0&\dfrac{\partial}{\partial X_2}\end{pmatrix}\begin{bmatrix}(\boldsymbol{\varPhi}^{\alpha})^{\mathrm{T}}&\boldsymbol{0}\\\boldsymbol{0}&(\boldsymbol{\varPhi}^{\alpha})^{\mathrm{T}}\end{bmatrix},\quad \boldsymbol{B}_2=\begin{bmatrix}\dfrac{\partial^2}{\partial X_1^2}&0\\0&\dfrac{\partial^2}{\partial X_1^2}\\\dfrac{\partial^2}{\partial X_1\partial X_2}&0\\0&\dfrac{\partial^2}{\partial X_1\partial X_2}\\\dfrac{\partial^2}{\partial X_2^2}&0\\0&\dfrac{\partial^2}{\partial X_2^2}\end{bmatrix}\begin{bmatrix}(\boldsymbol{\varPhi}^{\alpha})^{\mathrm{T}}&\boldsymbol{0}\\\boldsymbol{0}&(\boldsymbol{\varPhi}^{\alpha})^{\mathrm{T}}\end{bmatrix}\tag{A6}$$

$$\boldsymbol{D}_1=\begin{bmatrix}D_{11}&D_{12}&D_{13}\\D_{12}&D_{22}&D_{23}\\D_{13}&D_{23}&D_{33}\end{bmatrix},\quad \boldsymbol{D}_2=\begin{bmatrix}D_{11}&D_{12}&D_{13}&D_{13}&D_{23}&D_{33}\\D_{13}&D_{23}&D_{33}&D_{12}&D_{22}&D_{23}\end{bmatrix}\tag{A7}$$

$$\boldsymbol{S}=\begin{bmatrix}S_{11}\\S_{22}\\S_{12}\end{bmatrix},\quad \boldsymbol{S}_1=\begin{bmatrix}S_{11}&0&2S_{12}&0&S_{22}&0\\0&S_{11}&0&2S_{12}&0&S_{22}\end{bmatrix},\quad \boldsymbol{S}_2=\begin{bmatrix}S_{11}&0&S_{12}&0\\0&S_{12}&0&S_{22}\\S_{12}&0&S_{22}&0\\0&S_{11}&0&S_{12}\end{bmatrix}\tag{A8}$$

$$\boldsymbol{N}_1=\begin{bmatrix}N_1&0&N_2\\0&N_2&N_1\end{bmatrix},\quad \boldsymbol{N}_2=\begin{bmatrix}N_1&0&N_2&0\\0&N_2&0&N_1\end{bmatrix}\tag{A9}$$

$$\left.\begin{aligned}
&\boldsymbol{T}_1(\boldsymbol{S})=\begin{bmatrix}\dfrac{\partial}{\partial X_1} & 0 & \dfrac{\partial}{\partial X_1} & 0\\ 0 & \dfrac{\partial}{\partial X_1} & 0 & \dfrac{\partial}{\partial X_1}\end{bmatrix}\begin{bmatrix}S_{11} & & & \\ & S_{11} & & \\ & & S_{12} & \\ & & & S_{12}\end{bmatrix}\\
&\boldsymbol{T}_2(\boldsymbol{S})=\begin{bmatrix}\dfrac{\partial}{\partial X_2} & 0 & \dfrac{\partial}{\partial X_2} & 0\\ 0 & \dfrac{\partial}{\partial X_2} & 0 & \dfrac{\partial}{\partial X_2}\end{bmatrix}\begin{bmatrix}S_{12} & & & \\ & S_{12} & & \\ & & S_{22} & \\ & & & S_{22}\end{bmatrix}\\
&\boldsymbol{T}_3=\frac{\partial}{\partial X_1}\begin{bmatrix}S_{11}\\ S_{12}\end{bmatrix},\quad \boldsymbol{T}_4=\frac{\partial}{\partial X_2}\begin{bmatrix}S_{12}\\ S_{22}\end{bmatrix}
\end{aligned}\right\}\tag{A10}$$